Crossover from Symplectic to Orthogonal Class in a Two-Dimensional Honeycomb Lattice

Hidekatsu Suzuura* and Tsuneya Ando*

Institute for Solid State Physics, University of Tokyo, 5-1-5 Kashiwanoha, Kashiwa 277-8581, Japan

(Received 29 March 2002; published 12 December 2002)

We have calculated the weak-localization correction to the conductivity for disordered electrons in a two-dimensional honeycomb lattice and shown that it can be either positive or negative depending on the interaction range of impurity potentials. From symmetry considerations, the symplectic class turns out to be realized at nonzero temperatures and crossover to the orthogonal class is predicted with decreasing temperature.

DOI: 10.1103/PhysRevLett.89.266603 PACS numbers: 72.10.–d, 72.15.Rn, 73.20.Fz

A considerable number of studies have been made on carbon nanotubes since the discovery [1] and revealed that a metallic carbon nanotube is a ballistic conductor [2]. The ballistic conduction can be explained by suppression of backward scattering for conventional impurities [3,4]. Electronic properties of a carbon nanotube are explained by those of a two-dimensional (2D) graphite sheet consisting of a honeycomb lattice with the periodic boundary condition in a circumference direction [5]. Around half filling, equations of motion for electrons in a 2D honeycomb lattice are equivalent to Weyl equations for massless neutrinos giving linear dispersion relations [6]. This fact leads to the absence of backward scattering through destructive quantum interference due to the Berry phase of wavefunctions [7] and can give rise to various unusual properties. In this Letter, we focus on quantum electron transport, especially on Anderson-localization, in a 2D honeycomb lattice and study its universality class.

Recent progress in fabrication techniques of semiconductor microstructures enables us to realize artificial periodic potentials in a 2D electron system. A triangular lattice of closely arrayed antidots restricts electrons into the region composed of a honeycomb lattice. Therefore, the honeycomb lattice can be realized in such semiconductor microstructures as well as in 2D graphites.

From symmetry consideration, the universality class should be orthogonal without scattering due to magnetic impurities or spin-orbit interaction. On the other hand, negative interference mentioned above strongly suggests analogy with transport under spin-orbit interactions [8], and it leads to the fact that the system should belong to the symplectic class [9].

In this Letter, we explicitly calculate weak-localization (WL) corrections to the Boltzmann conductivity due to random potentials and show that the correction can be either positive or negative depending on the interaction range of scattering potentials. In addition, we discuss the universality class from time-reversal and pseudospin-rotational symmetries [10] and show that crossover between symplectic and orthogonal class takes place.

A unit cell of a honeycomb lattice contains two sublattices. Each sublattice is usually called an A or B site, respectively, and this internal degree of freedom plays a role of a pseudospin. Moreover, the Fermi surface of a half-filled honeycomb lattice consists of two points called K and K' points in the first Brillouin zone, and a valley index is necessary to specify electrons around the Fermi energy. As a result, conducting electrons have another species of pseudospin with regard to the valley index. Note that we have not considered true electron spin throughout this study for simplicity.

Pauli matrices are introduced for the sublattice index as $\vec{\sigma} = (\sigma^x, \sigma^y, \sigma^z)$, regarding the A (B) site as an up (down) spin, and for the valley index as $\vec{\tau} = (\tau^x, \tau^y, \tau^z)$, regarding the K (K') point as an up (down) spin. Eigenstates for up and down spins are described by $|+\rangle$ and $|-\rangle$, respectively.

The Hamiltonian for slowly varying envelope functions around two Fermi points within the effective-mass approximation is given by [6]

$$\mathcal{H}_0 = \gamma[\hat{k}_x(\sigma^x \otimes \mathbf{1}_2) + \hat{k}_y(\sigma^y \otimes \tau^z)], \tag{1}$$

where γ denotes the band parameter, $\hat{k}_x$ and $\hat{k}_y$ are wave-number operators, and $\mathbf{1}_2$ is the identity matrix of rank 2. Eigenstates in a $\boldsymbol{k}$ representation are accompanied by the product of two pseudospin states

$$|js\boldsymbol{k}\rangle = |\boldsymbol{k}\rangle\left[\frac{1}{\sqrt{2}}(s|j\rangle + e^{i\varphi_k}|-j\rangle) \otimes |j\rangle\right], \tag{2}$$

with the valley index j, which is $+$ for K and $-$ for K', and with the band index s, $+$ for a conduction band and $-$ for a valence band, where $e^{i\varphi_k} = (k_x + ik_y)/|k_x + ik_y|$ and its eigenenergy is given by $\varepsilon_{js\boldsymbol{k}} = s\gamma k$ with $k = |\boldsymbol{k}|$. Hereafter, we simplify the notation as $|\alpha\rangle = |js\boldsymbol{k}\rangle$.

The key point in this study is the interaction range of a random potential. Conventional impurities cause no intervalley scattering, and intravalley scatterings at A and B sublattices give little difference. Their potential is represented by

$$\mathcal{U}^L = \sum_n u_n^L (\mathbf{1}_2 \otimes \mathbf{1}_2)\delta(\hat{\boldsymbol{r}} - \boldsymbol{r}_n^L), \tag{3}$$

where the spatial dependence is replaced by the delta function because the Fermi wavelength of conducting electrons is assumed to be much larger than the characteristic length of potential variation. As a matter of convenience, this is called long-range potential though only a lattice spacing is long enough for interaction range to represent a potential by Eq. (3) [11].

Intervalley scattering is induced by potentials with extremely short interaction range like a lattice vacancy. In a short-range limit, the potential is localized either at an A or at a B sublattice and intravalley scattering is generated as much. Consider that intervalley scattering is accompanied by the phase shift $\phi(\boldsymbol{r}) = (\boldsymbol{K}' - \boldsymbol{K}) \cdot \mathbf{r}$ from Bloch functions of initial and final states, and the short-range impurity potential is given by

$$\begin{aligned} \mathcal{U}^S &= \mathcal{U}^+ + \mathcal{U}^-, \\ \mathcal{U}^\pm &= \sum_n u_n^\pm \{P^\pm \otimes [\mathbf{1}_2 + \vec{e}(\boldsymbol{r}_n^\pm) \cdot \vec{\tau}]\}\delta(\hat{\boldsymbol{r}} - \boldsymbol{r}_n^\pm), \end{aligned} \tag{4}$$

where $P^\pm = (\mathbf{1}_2 \pm \sigma^z)/2$, $\vec{e}(\boldsymbol{r}) = (\cos\phi(\boldsymbol{r}), \sin\phi(\boldsymbol{r}), 0)$, and $\mathcal{U}^\pm$ represents the potential of the impurities localized at A or B sublattices, respectively. The effective-mass theory with the potential given above well explains the conductance quantization of carbon nanotubes with a lattice vacancy [12,13].

We calculate conductivity by the Kubo formula and perform perturbative expansion in terms of the random potential $\mathcal{U}$ within the Born approximation taking ensemble average of randomly distributed scatterers. Figure 1(a) gives the diagram of the Boltzmann conductivity for isotropic scattering potential

$$\sigma_{xx}^0 = \frac{e^2\hbar}{2\pi S} \sum_{\alpha\alpha'} v_{\alpha\alpha'}^x G_{\alpha'}^+(\varepsilon_F) v_{\alpha'\alpha}^x G_\alpha^-(\varepsilon_F), \tag{5}$$

where S denotes the area of the system, $v_{\alpha\alpha'}^x = \langle\alpha|\hat{\boldsymbol{v}}^x|\alpha'\rangle$, impurity-averaged Green's functions are defined by

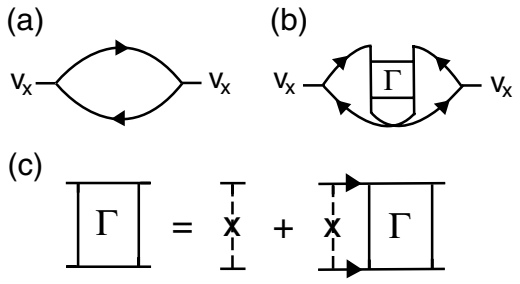

FIG. 1. Diagrams for calculations of conductivity by Kubo formula: (a) Boltzmann conductivity, (b) weak-localization correction, and (c) Bethe-Salpeter equation for vertex function Γ. A line with an arrow represents an impurity-averaged Green function. A dashed line with a cross shows an averaged product of two impurity potentials, or a bare vertex function.

$G_\alpha^\pm(\varepsilon) = [\varepsilon - \varepsilon_\alpha \pm i\hbar/2\tau_\alpha(\varepsilon)]^{-1}$, and the relaxation time is given by

$$\frac{1}{\tau_\alpha(\varepsilon)} = \frac{2\pi}{\hbar} \sum_{\alpha'} \langle |U_{\alpha'\alpha}|^2 \rangle_{\text{imp}} \delta(\varepsilon - \varepsilon_{\alpha'}), \tag{6}$$

using the matrix element of potential, $U_{\alpha'\alpha} = \langle\alpha'|\mathcal{U}|\alpha\rangle$. The velocity operator is defined as

$$\hat{\boldsymbol{v}}^x = \frac{1}{i\hbar}[\hat{x}, \mathcal{H}_0] = v_F(\sigma^x \otimes \mathbf{1}_2), \tag{7}$$

with $v_F = \gamma/\hbar$. The ensemble average denoted by $\langle\cdots\rangle_{\text{imp}}$ is taken over all possible configurations of random potentials.

Before evaluating WL corrections, it is worth noting that quantum fluctuation breaks down the lowest Born approximation for the relaxation time around $\varepsilon_F = 0$. In fact, the conductivity is strongly suppressed at $\varepsilon_F = 0$ and shows singular behavior around there according to the self-consistent Born approximation [14,15]. In this Letter, ε_F is assumed to be large enough to avoid such a singular behavior and to clarify WL effects due to quantum interference. This assumption makes scattering between conduction and valence bands negligible and the band index s can be fixed to $+$, which is omitted in the following calculations. Then, the velocity operator becomes diagonal, $v_{\alpha\alpha'}^x = \langle j + \boldsymbol{k}|\hat{\boldsymbol{v}}^x|j' + \boldsymbol{k}'\rangle = \delta_{\alpha\alpha'} v_\alpha^x$ with $v_\alpha^x = v_F \cos\varphi_{\boldsymbol{k}}$.

For quantum corrections to the Boltzmann conductivity we collect what is called maximally crossed diagrams [16,17]. As shown in Fig. 1(b) the sum of them is expressed as

$$\Delta\sigma_{xx} = \frac{e^2\hbar}{2\pi S} \sum_{\alpha\alpha'} v_\alpha^x G_\alpha^+ G_\alpha^- \Gamma_{\alpha\alpha'\alpha'\alpha} G_{\alpha'}^+ G_{\alpha'}^- v_{\alpha'}^x, \tag{8}$$

using the vertex function $\Gamma_{\beta\beta'\alpha\alpha'}$, where the dependence on ε_F is not explicitly shown. Figure 1(c) graphically shows the Bethe-Salpeter equation for $\Gamma_{\beta\beta'\alpha\alpha'}$,

$$\Gamma_{\beta\beta'\alpha\alpha'} = \Gamma^0_{\beta\beta'\alpha\alpha'} + \sum_{\mu\mu'} \Gamma_{\beta\beta'\mu\mu'} G_\mu^+ G_{\mu'}^- \Gamma^0_{\mu\mu'\alpha\alpha'}, \tag{9}$$

where the bare vertex is defined as $\Gamma^0_{\beta\beta'\alpha\alpha'} = \langle U_{\beta\alpha} U_{\beta'\alpha'} \rangle_{\text{imp}}$. Owing to momentum conservation, the following $\boldsymbol{q}$ and J become constant,

$$\begin{aligned} \boldsymbol{q} &= \boldsymbol{k}_\alpha + \boldsymbol{k}_{\alpha'} = \boldsymbol{k}_\mu + \boldsymbol{k}_{\mu'} = \boldsymbol{k}_\beta + \boldsymbol{k}_{\beta'}, \\ J &= j_\alpha + j_{\alpha'} = j_\mu + j_{\mu'} = j_\beta + j_{\beta'}. \end{aligned} \tag{10}$$

Note that conservation of J originates in the condition $|\boldsymbol{K} - \boldsymbol{K}'| \gg k$. As a result, Eq. (9) is decoupled into three sectors of $J = 0$ and ± 2, and, hereafter, the vertex function is described as $\Gamma_{\alpha\beta}(\boldsymbol{q}, J) = \Gamma_{\beta\beta'\alpha\alpha'}$.

In the limit of $q \to 0$, the vertex function has divergent contributions $\propto q^{-2}$ and generates logarithmic corrections to the Boltzmann conductivity for 2D systems, and this is also the case with a 2D honeycomb lattice containing multivalleys.

Previous studies on the quantum corrections for noninteracting electrons in multivalley systems show nothing but slight modifications to give quantitative evaluation [18–20]. However, it turns out that the potential which induces intervalley scattering plays a crucial role and can change the sign of the quantum corrections as shown in the following.

First, we consider the system with long-range potentials. With no short-range potential, the index j can also be omitted and $\boldsymbol{k}$ is a unique index to specify a one-particle state because intervalley scattering is suppressed. The relaxation time is given by [14]

$$\frac{1}{\tau} = \frac{nu^2}{2\hbar\gamma^2}\varepsilon_F, \tag{11}$$

where n is the concentration of impurities, $nu^2 = \sum_i (u_i^L)^2/S$. The Boltzmann conductivity is given by

$$\sigma_{xx}^0 = \frac{e^2}{2\pi\hbar}\left(\frac{\varepsilon_F \tau_{tr}}{\hbar}\right) = \frac{e^2}{2\pi\hbar} k_F \ell, \tag{12}$$

where $k_F = \varepsilon_F/\gamma$ and $\ell = v_F \tau_{tr}$. For the long-range potential it is necessary to add vertex corrections given by the integral equation as shown in Fig. 2, which doubles the conductivity [14]. In other words, the transport relaxation time τ_{tr} is different from τ and, in this case, $\tau_{tr} = 2\tau$.

Under the conditions that q/k_F is neglected, the bare vertex function is given by

$$\Gamma^0_{\boldsymbol{k}_\alpha \boldsymbol{k}_\beta}(\boldsymbol{q}) = \frac{nu^2}{2S} e^{i(\varphi_{\boldsymbol{k}_\alpha} - \varphi_{\boldsymbol{k}_\beta})}[1 + \cos(\varphi_{\boldsymbol{k}_\alpha} - \varphi_{\boldsymbol{k}_\beta})]. \tag{13}$$

The phase factor $e^{i(\varphi_{\boldsymbol{k}_\alpha} - \varphi_{\boldsymbol{k}_\beta})}$ originates from the Berry phase of eigenfunctions which causes the suppression of backward scattering [7]. The angular dependence except the phase factor is generated by the anisotropy in scattering. We solve Eq. (10) iteratively and collect the most divergent contributions in the limit of $q \to 0$

$$\Gamma_{\boldsymbol{k}_\alpha \boldsymbol{k}_\beta}(\boldsymbol{q}) = \frac{nu^2}{2S} e^{i(\varphi_{\boldsymbol{k}_\alpha} - \varphi_{\boldsymbol{k}_\beta})} \frac{1}{(v_F \tau q)^2}, \tag{14}$$

To get the vertex function in Eq. (8), we put $\beta = \alpha'$, or $\boldsymbol{k}_\beta = \boldsymbol{k}_{\alpha'} = \boldsymbol{q} - \boldsymbol{k}_\alpha$, giving $e^{i(\varphi_{\boldsymbol{k}_\alpha} - \varphi_{\boldsymbol{k}_\beta})} = -1 + O(q/k_F)$. This factor of -1 makes the vertex part negative, and we obtain positive WL correction

$$\Delta\sigma_{xx} = \frac{2e^2}{\pi^2\hbar} \ln\left(\frac{\ell_\phi}{\ell}\right), \tag{15}$$

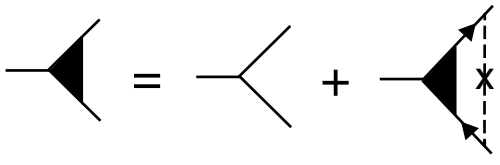

FIG. 2. Diagrams for the integral equation giving vertex corrections.

considering the degeneracy of two Fermi points and vertex corrections to maximally crossed diagrams at both vertices. Here we assume that, in q summation, the upper cutoff is the inverse of the elastic scattering length, ℓ^{-1}, and the lower one the inverse of the phase-coherence length, ℓ_ϕ^{-1}. Because of the Berry phase, the correction becomes positive, showing antilocalization behavior.

In contrast, for short-range potentials, the index j becomes necessary because this is no longer a conserved quantity. In spite of intervalley scattering, the relaxation time is the same as that for the system with long-range potentials provided that $nu^2 = [\sum_i (u_i^+)^2 + \sum_i (u_i^-)^2]/S$ and, what is more, potentials are assumed to be distributed uniformly at A and B sites, or $\sum_i (u_i^+)^2 = \sum_i (u_i^-)^2$. Now that vertex corrections give no contributions, $\tau_{tr} = \tau$ and the Boltzmann conductivity becomes half of that for long-range potentials.

As for the vertex function, only the sector with $J = 0$ makes divergent contributions for short-range potentials. The bare vertex is written as

$$\Gamma^0_{\alpha\beta}(\boldsymbol{q}, 0) = \frac{nu^2}{4S} j_\alpha j_\beta e^{i(\varphi_{\boldsymbol{k}_\alpha} - \varphi_{\boldsymbol{k}_\beta})}, \tag{16}$$

where $j_\alpha j_\beta$ appears and $\cos(\varphi_{\boldsymbol{k}_\alpha} - \varphi_{\boldsymbol{k}_\beta})$ disappears compared to that of long-range potential. We obtain a divergent solution of Eq. (9) in the limit of $q \to 0$

$$\Gamma_{\alpha\beta}(\boldsymbol{q}, 0) = \frac{nu^2}{2S} j_\alpha j_\beta e^{i(\varphi_{\boldsymbol{k}_\alpha} - \varphi_{\boldsymbol{k}_\beta})} \frac{1}{(v_F \tau q)^2}. \tag{17}$$

Considering $j_\beta = j_{\alpha'} = -j_\alpha$, we get an additional factor $j_\alpha j_\beta = -1$. Consequently, the vertex function becomes positive and Eq. (8) is calculated as

$$\Delta\sigma_{xx} = -\frac{e^2}{2\pi^2\hbar} \ln\left(\frac{\ell_\phi}{\ell}\right), \tag{18}$$

which shows normal WL.

The preceding results naturally bring up the following question. What happens in the system with both types of potentials? Here we briefly show calculated results. The vertex function in the sector $J = \pm 2$ remains finite as long as short-range potential exists, no matter how weak it is. On the other hand, the vertex in the sector $J = 0$ is always divergent and positive even if long-range potential exists.

Hereafter, we discuss the universality class considering fundamental symmetry of the Hamiltonian and compare the result to WL corrections calculated above. Recently, disordered systems have been classified into ten universality classes including the standard three with the random-matrix theory taking particle-hole symmetry into account [21]. In this study, however, it is not necessary to consider such new classes because diagonal random potentials break particle-hole symmetry. Further, due to time-reversal symmetry, the system should belong either to the orthogonal or to the symplectic class.

In the original system without true spins the time-reversal operator $\mathcal{T}$ is simply given by the

complex-conjugation C. In our effective-mass theory, considering that Bloch functions at K and K' points are complex conjugate to each other, $\mathcal{T}$ is given by

$$\mathcal{T} = (\sigma_z \otimes \tau_x)C, \tag{19}$$

which commutes with $\mathcal{H}_0$, $\mathcal{U}^S$, and $\mathcal{U}^L$. In this case, a unitary transformation brings $\mathcal{T}$ to C [10]. Thus, no extra symmetry is indicated and the system belongs to the orthogonal class.

Without short-range potentials, electrons around each Fermi point become independent and there appears another symmetry defined by the operator

$$\tilde{\mathcal{T}} = -i(\sigma_y \otimes \mathbf{1}_2)C, \tag{20}$$

which commutes with $\mathcal{H}_0$ and $\mathcal{U}^L$ but not with $\mathcal{U}^S$. This operator $\tilde{\mathcal{T}}$ transforms $|js\boldsymbol{k}\rangle$ into $|js - \boldsymbol{k}\rangle$ and is regarded as time-reversal operation for transport under intravalley scattering. There is a definitive difference between these operators for double operations: $\mathcal{T}^2 = 1$ and $\tilde{\mathcal{T}}^2 = -1$. Clearly, $\tilde{\mathcal{T}}$ cannot be reduced to C and Kramers degeneracy inevitably happens. Therefore, the symplectic class should be considered.

In view of pseudospin-rotational symmetry, this model is regarded as an integer-spin system containing two species of pseudospins with $S = 1/2$ and short-range potentials certainly break rotational symmetry for both spins. So it is classified into the orthogonal class [10]. For long-range potentials, however, the pseudospin with regard to two separate Fermi points is a conserved quantity and must first be eliminated. This is a system with half-odd-integer spin, and rotational invariance for another pseudospin of the sublattice index is broken by intravalley-potential scattering. Therefore the system belongs to the symplectic class without short-range potentials.

These symmetry considerations are consistent with calculated WL corrections. It should be emphasized that the symplectic class, or antilocalization, can be realized without spin-orbit interaction.

Here we should point out that crude symmetry considerations can easily lead us to incorrect universality classes. For example, purely two-dimensional electrons with spin-orbit scattering on impurities belong not to the symplectic but to the unitary class [9]. In the present model without intervalley scattering, the same situation is brought about by the potential proportional to $\sigma_z \otimes \mathbf{1}_2$ that does not commute with $\tilde{\mathcal{T}}$.

Discussions above show that the short-range potential drives the system into the orthogonal class *at zero temperature*. In realistic systems, it seems quite reasonable to assume that the elastic scattering length determined by the short-range potential is much longer than that by the long-range potential, or $\ell_S \gg \ell_L$. This is confirmed by numerical calculations and by the ballistic transport experimentally realized in carbon nanotubes as mentioned first. Therefore, at nonzero temperature, antilocalization behavior, or logarithmically increasing conductivity should be observed with decreasing temperature as long as $\ell_L \ll \ell_\phi \ll \ell_S$. When temperature is quite low and $\ell_S \simeq \ell_\phi$, the conductivity turns into decrease toward zero temperature. That is to, say, electrons in a 2D honeycomb lattice belong to the symplectic class at nonzero temperature and crossover from symplectic to orthogonal class takes place at quite low temperature.

This work has been supported in part by Grants-in-Aid for COE (12CE2004 "Control of Electrons by Quantum Dot Structures and Its Application to Advanced Electronics") and Scientific Research from the Ministry of Education, Science and Culture, Japan.

*Present address: Department of Physics, Tokyo Institute of Technology, 2-12-1 Ookayama, Meguro-ku, Tokyo 152-8551, Japan.

[1] S. Iijima, Nature (London) **354**, 56 (1991).
[2] S. J. Tans, M. H. Devoret, H. Dai, A. Thess, R. E. Smalley, L. J. Geerligs, and C. Dekker, Nature (London) **386**, 474 (1997).
[3] T. Ando and T. Nakanishi, J. Phys. Soc. Jpn. **67**, 1704 (1998).
[4] P. L. McEuen, M. Bockrath, D. H. Cobden, Y.-G. Yoon, and S. G. Louie, Phys. Rev. Lett. **83**, 5098 (1999).
[5] R. Saito, G. Dresselhaus, and M. S. Dresselhaus, *Physical Properties of Carbon Nanotubes* (Imperial College Press, London, 1998).
[6] J. C. Slonczewski and P. R. Weiss, Phys. Rev. **109**, 272 (1958).
[7] T. Ando, T. Nakanishi, and R. Saito, J. Phys. Soc. Jpn. **67**, 2857 (1998).
[8] G. Bergmann, Phys. Rep. **107**, 1 (1984).
[9] S. Hikami, A. I. Larkin, and Y. Nagaoka, Prog. Theor. Phys. **63**, 707 (1980).
[10] F. J. Dyson, J. Math. Phys. (N.Y.) **3**, 140 (1962).
[11] T. Nakanishi and T. Ando, J. Phys. Soc. Jpn. **68**, 561 (1999).
[12] M. Igami, T. Nakanishi, and T. Ando, J. Phys. Soc. Jpn. **68**, 716 (1999); **68**, 3146 (1999).
[13] T. Ando, T. Nakanishi, and M. Igami, J. Phys. Soc. Jpn. **68**, 3994 (1999).
[14] N. H. Shon and T. Ando, J. Phys. Soc. Jpn. **67**, 2421 (1998).
[15] T. Ando, Y. Zheng, and H. Suzuura, J. Phys. Soc. Jpn. **71**, 1318 (2002).
[16] L. G. Gor'kov, A. I. Larkin, and D. E. Khmel'nitskii, Pis'ma Zh. Eksp. Teor. Fiz. **30**, 248 (1979) [JETP Lett. **30**, 228 (1979)].
[17] E. Abrahams, P.W. Anderson, D. C. Licciardello, and T.V. Ramakrishnan, Phys. Rev. Lett. **42**, 673 (1979).
[18] A. Kawabata, J. Phys. Soc. Jpn. **49**, 628 (1980).
[19] H. Fukuyama, Prog. Theor. Phys. Suppl. **69**, 220 (1980).
[20] B. L. Alt'shuler, A. G. Aronov, A. I. Larkin, and D. E. Khmel'nitskii, Zh. Eksp. Teor. Fiz. **81**, 768 (1981) [Sov. Phys. JETP **54**, 411 (1981)].
[21] M. R. Zirnbauer, J. Math. Phys. (N.Y.) **37**, 4986 (1996).